Inorg. Chem. **2006**, *45*, 10180–10187

Inorganic Chemistry
Article

Dinuclear Gold(I) Isocyanide Complexes with Luminescent Properties, and Displaying Thermotropic Liquid Crystalline Behavior

Silverio Coco,* Carlos Cordovilla, Pablo Espinet,* José Martín-Álvarez, and Paula Muñoz

Química Inorgánica, Facultad de Ciencias, Universidad de Valladolid, E-47005 Valladolid, Spain

Received April 25, 2006

Dinuclear gold(I) complexes [μ-(4,4′-CN-R-NC){Au($C_6F_4OC_4H_9$)}$_2$] [R = 1,4-phenylene, $n = 8$; R = 4,4′-biphenylene, 2,2′-dichloro-4,4′-biphenylene, 2,2′-dimethyl-4,4′-biphenylene, n = 4,6,8,10] have been prepared and their liquid crystal behavior and optical properties studied. Although the free ligands are not mesomorphic, all the gold(I) derivatives described, except the phenylisonitrilegold(I) derivative [μ-(1,4-CN-C_6H_4-NC){Au($C_6F_4OC_8H_{17}$)}$_2$], display liquid crystal behavior, giving rise to a nematic mesophase. The transition temperatures decrease in the order 4-4′-biphenylene > 2,2′-dichloro-4-4′-biphenylene > 2,2′dimethyl-4-4′-biphenylene. All compounds show photoluminescence in the solid state and in solution. The single-crystal X-ray diffraction structures of [μ-(4,4′-CN-R-NC)-{Au($C_6F_4OC_nH_{2n+1}$)}$_2$] (R = 4-4′-biphenylene and 2,2′-dichloro-4-4′-biphenylene) have been determined confirming the rodlike structure of the molecule, with a linear coordination around the gold atoms. There are Au•••Au interactions in the 2,2′-dichlorobiphenyl derivative but not in the 4-4′-biphenyl compound.

Introduction

One reason for the interest in the preparation and study of liquid crystals with metal-containing molecules (metallomesogens) is connected to the possibility of combining the properties of mesogenic systems (supramolecular organization and fluidity in the mesophase) with those of transition or post-transition metals (high birefringence, paramagnetism, or color).[1−6] In this respect, the incorporation of emission properties into liquid crystals is currently an important area of research, as this type of system is particularly suitable for the development of novel liquid crystalline displays.[7] A number of luminescent liquid crystals based on organic molecules have been reported,[8−14] but just a few metal-containing molecules giving rise to mesophases (metallomesogens) and displaying luminescent properties have been described: These include a few palladium complexes,[15] some lanthanide derivatives,[7,16−19] and recently a family of tetrafluoroarylgold(I) isocyanide complexes, which show strong photoluminescence in the mesophase, as well as in the solid state and in solution.[20] So far, only the two latter references report luminescence in the mesophase.

An important goal in this area of research is to establish a clear structure−luminescence relationship, but we are still far from predicting and controlling these properties. Numerous studies have suggested that aurophilic interactions play

---

* To whom correspondence should be addressed. E-mail: espinet@qi.uva.es (P.E.).

(1) Espinet P.; Esteruelas, M. A.; Oro, L. A.; Serrano, J. L.; Sola, E. *Coord. Chem. Rev.* **1992**, *117*, 215.
(2) *Metallomesogens*; Serrano, J. L., Ed.; VCH: Weinheim, 1996.
(3) Bruce, D. W. *Inorganic Materials*, 2nd ed.; Bruce, D. W., O'Hare, D., Eds.; Wiley: Chichester 1996; Chapter 8. (b) Donnio, B.; Bruce, D. W. *Struct. Bonding* **1999**, *95 (Liquid Crystals II)*, 193.
(4) Espinet, P. *Gold Bull.* **1999**, *32*, 127.
(5) Collings, P. J. *Liquid Crystals (Nature's Delicate Phase of Matter)*; Princeton University Press: Princeton, NJ, 1990.
(6) *Handbook of Liquid Crystals*; Demus, D., Goodby, J., Gray, G. W., Spiess, H. W., Vill, D. V., Eds.; Wiley-VCH: Weinheim, 1998.
(7) Guillet, E.; Imbert, D.; Scopelliti, R.; Bünzli, J.-C. G. *Chem. Mater.* **2004**, *16*, 4063.
(8) Yu, L. J.; Labes, M. M. *Appl. Phys. Lett.* **1977**, *279*, 835.
(9) Zhang, Y.; Zhu, W.; Wang, W.; Tian, H.; Su, J.; Wang, W. *J. Mater. Chem.* **2002**, *12*, 1294.
(10) Hoag, B. P.; Gin, D. L. *Adv. Mater.* **1998**, *10*, 1546.
(11) Boardman, F. H.; Dunmur, D. A.; Grossel, M. C.; Luckhurst, G. R. *Chem. Lett.* **2002**, 60.
(12) Attias, A.-J.; Cavalli, C.; Donnio, B.; Guillon, D.; Hapiot, P.; Malthête, J. *Chem. Mater.* **2002**, *14*, 375.
(13) Zhang, Y.; Zhu, W.; Wang, W.; Tian, H.; Su, J.; Wang, W. *J. Mater. Chem.* **2002**, *12*, 1294.
(14) Pschirer, N. G.; Vaughn, M. E.; Dong, Y. B.; zur Loye, H.-C.; Bunz, U. H. F. *Chem. Commun.* **2000**, 85.
(15) Neve, F.; Ghedini, M.; Crispini, A. *Chem. Commun.* **1996**, 2463. (b) Ghedini, M.; Aiello, I.; La Deda, M.; Grisolia, A. *Chem. Commun.* **2003**, 2198.
(16) Binnemans K.; Görller-Walrand, C. *Chem. Rev.* **2002**, *102*, 2303.
(17) Galyametdinov, Y. G.; Ivanova, G. I.; Ovchinnikov, I. V. *Bull. Acad. Sci. USSR, Div. Chem. Sci.* **1991**, *40*, 1109.
(18) Binnemans K.; Galyametdinov, Y. G.; Collison, S. R.; Bruce, D. W. *J. Mater. Chem.* **1998**, *8*, 1551.
(19) Suárez, S.; Mamula, O.; Imbert, D.; Piguet, C.; Bünzli, J.-C. G. *Chem. Commun.* **2003**, 1226.
(20) Bayón, R.; Coco, S.; Espinet, P. *Chem. Eur. J.* **2005**, *11*, 1079.

10.1021/ic060702a CCC: $33.50

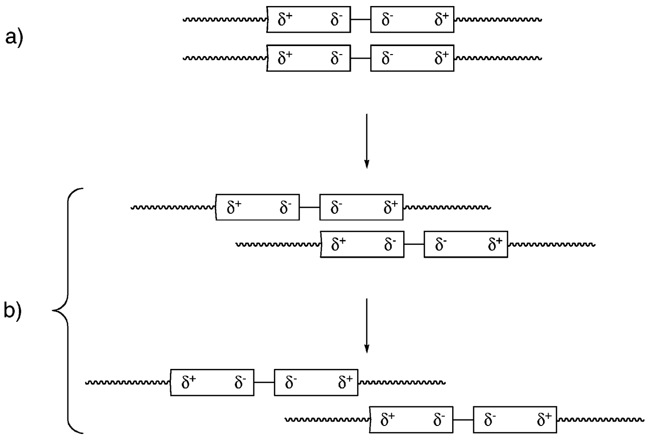

Figure 1. A simple model suggesting how, in symmetric dimers, the best multipole−multipole interactions are not those arising from layered packing of molecules, represented in part a, but those involving some mixing of aromatic and aliphatic regions, represented in part b (see also ref 23).

a key role in the luminescence of gold(I) complexes.[21] Au···Au intermolecular interactions have also been proposed to be important for the mesogenic behavior of simple gold alkylisocyanide complexes.[22] However, these interactions are not always needed. For instance, the tetrafluoroarylgold(I) isocyanide derivatives mentioned above show two phosphorescent emissions in the solid state that disappear in solution. A single-crystal X-ray diffraction study of one of these tetrafluorophenylgold complexes demonstrated the absence of Au···Au contacts in the solid state. Moreover, well-defined intermolecular $F_{ortho}\cdots F_{meta}$ interactions were found, which are responsible for the crystal packing. A detailed study proved that the photoluminescence observed has an intramolecular origin and is not associated with any Au···Au contacts.[20]

We have reported previously a family of dinuclear organometallic gold complexes $[(\mu\text{-}4,4'\text{-}C_6F_4C_6F_4)\{AuCN\text{-}(C_6H_4)_mOC_nH_{2n+1}\}_2]$ with unusual mesogenic behavior: Although they display high transition temperatures, indicating strong intermolecular interactions, they give rise only to a nematic phase, and not to more ordered mesophases.[23] This apparent contradiction (strong interactions but only a less ordered mesophase) was explained considering the electronic and structural factors that determine the intermolecular interactions in the system. It was suggested, but not experimentally confirmed, that in these molecules with large twist angles between the two rings of the octafluorobiphenyl group the best multipole−multipole interactions should involve a not layered packing structure (Figure 1), whether in the solid or in the mesophase. As a consequence, only a nematic phase might appear above the melting point.

We therefore decided to synthesize similar dinuclear tetrafluorophenyl gold(I) complexes of type $[\mu\text{-}(4,4'\text{-CN-R-NC})\{Au(C_6F_4OC_nH_{2n+1})\}_2]$, containing a diisocyanide ligand bringing group two gold atoms. The selection of diisocyanides was directed to have a set of ligands containing a rigid aromatic core (R = C_6H_4 or biphenylenes) with different twist angles between the two rings of the biphenyl group, to check experimentally their influence on the properties of the system. Here we report the synthesis and complete characterization of a family of dinuclear metallomesogens displaying only a nematic mesophase and intense luminescence at room temperature, including the study of two crystal structures of $[\mu\text{-}(4,4'\text{-CN-R-NC})\{Au(C_6F_4OC_4H_9)\}_2]$ (R = 4,4′-biphenylene and 2,2′-dichloro-4,4′-biphenylene; we could not get good quality crystals for R = 2,2′-dimethyl-4,4′-biphenylene).

Experimental Section

Combustion analyses were made with a Perkin-Elmer 2400 microanalyzer. IR spectra (cm^{-1}) were recorded on a Perkin-Elmer FT 1720X instrument and ^1H and ^{19}F NMR spectra on Bruker AC 300 or ARX 300 instruments in $CDCl_3$. Microscopy studies were carried out using a Leica DMRB microscope equipped with a Mettler FP82HT hot stage and a Mettler FP90 central processor, at a heating rate of 10 °C min^{-1}. For differential scanning calorimetry (DSC) a Perkin-Elmer DSC7 instrument was used, which was calibrated with water and indium. The scanning rate was 10 °C min^{-1}, the samples were sealed in aluminum capsules in the air, and the holder atmosphere was dry nitrogen. UV−vis absorption spectra were obtained on a Shimadzu UV-1603 spectrophotometer in dichloromethane solutions (1×10^{-4} M). Luminescence data were recorded on a Perkin-Elmer LS-55 luminescence spectrometer. Luminiscence quantum yields were obtained at room temperature using the optically dilute method in degassed dichloromethane (quantum yields standard was quinine sulfate in 0.1 N aqueous sulfuric solution $\Phi = 0.546$).[24]

Literature methods were used to prepare 1-alkyloxy-2,3,5,6-tetrafluorobenzenes.[25] 1,4-diisocyanobenzene,[26] 4,4′-diisocyanobiphenyl,[26] 2,2′-dichloro-4,4′-dinitrobiphenyl,[27] 4,4′-diamino-2,2′-dimethylbiphenyl,[28] and [AuCl(tht)] (tht = tetrahydrothiophene).[29]

Only typical examples are described, as the syntheses were similar for the rest of the compounds. Yields, IR, and analytical data are given for all the gold complexes.

CAUTION!: Aminobiphenyls are very carcinogenic materials and must be handled with extreme care.

Preparation of 4,4′-Diamino-2,2′-dichlorobiphenyl. Graphite (2.0 g) was added to a solution of 2,2′-dichloro-4,4′-dinitrobiphenyl (0.63 g, 2.01 mmol) and hydrazine monohydrate (1.36 mL, 28.16 mmol) in 50 mL of dried ethanol. The flask was purged with N_2, and the suspension was refluxed for 6 h. The reaction mixture was allowed to cool to 40 °C and filtered. The solvent was removed on a rotary evaporator to obtain the product as white solid (80.5 g, 98% yield).

Preparation of 2,2′-Dichloro-4,4′-diisocyanobiphenyl. The procedure described by Ugi was followed, but with triphosgene as

---

(21) White-Morris, R. L.; Olmstead, M. M.; Balch, A. L. *J. Am. Chem. Soc.* **2003**, *125*, 1033.
(22) Bachman, R. E.; Fioritto, M. S.; Fetics, S. K.; Cocker, T. M. *J. Am. Chem. Soc.* **2001**, 123, 5376.
(23) Bayón, R.; Coco, S.; Espinet, P.; Fernández-Mayordomo, C.; Martín-Álvarez, J. M. *Inorg. Chem.* **1997**, *36*, 2329.
(24) Melhuish, W. H. *J. Phys. Chem.* **1961**, *65*, 229.
(25) Coco, S.; Fernández- Mayordomo, C.; Falagán, S. Espinet, P. *Inorg. Chim. Acta* **2003**, *350*, 366.
(26) Efraty, A.; Feinstein, I.; Wackerle, L.; Goldman, A. *J. Org. Chem.* **1980**, *45*, 4059.
(27) Lñitunenko, L. M.; Grekov, A. P.; Verkhovod, N. N.; Dzyuba, U. P. *Chem. Abstr.* **1957**, *51*, 5007.
(28) Calin, R. B.; Odioso, R. C. *J. Am. Chem. Soc.* **1954**, *76*, 2345.
(29) Usón, R.; Laguna, A.; Vicente, J. *J. Organomet. Chem.* **1977**, *131*, 471.

dehydrating agent.[30] To a solution of 4,4′-di-*N*-formamido-2,2′-dichlorobiphenyl (0.6 g, 1.94 mmol), prepared by reaction of the diamine with formic acid, and triethylamine (1.08 mL, 7.76 mmol) in 50 mL of CH_2Cl_2 was added dropwise a solution of trichloromethyl carbonate (triphosgene) (0.69 g, 2.32 mmol) in 25 mL of CH_2Cl_2. The mixture was refluxed for 2 h, and then, the solvent was removed on a rotary evaporator. The resulting residue was chromatographed (silica gel, CH_2Cl_2/hexane, 3:1 as eluent), and the solvent was evaporated to obtain the product as a white solid (0.34 g, 64% yield). IR $\nu(C{\equiv}N)/(CH_2Cl_2)$: 2130 cm^{-1}. ^1H NMR ($CDCl_3$): δ_A 7.55 (d, 2H, $J_{AM} = 1.8$ Hz), δ_M 7.38 (dd, 2H, $J_{MX} =$ 8.2 Hz), $J_{AM} = 1.8$ Hz), δ_X 7.29 (d, 2H, $J_{MX} = 8.2$ Hz).

Preparation of 2,2′-Dimethyl-4,4′-diisocyanobiphenyl. This isonitrile was prepared as described for the analogous 2,2′-dichloro-4,4′-diisocyanobiphenyl, starting from 4,4′-diamino-2,2′-dimethylbiphenyl. IR $\nu(C{\equiv}N)/(CH_2Cl_2)$: 2126 cm^{-1}. ^1H NMR ($CDCl_3$): δ_A 7.31 (d, 2H, $J_{AM} = 1.7$ Hz), δ_M 7.27 (dd, 2H, $J_{MX} = 8.0$ Hz, $J_{AM} = 1.7$ Hz), δ_X 7.07 (d, 2H, $J_{MX} = 8.0$ Hz), 2.03 (s, 6H, CH_3).

Preparation of [μ-(4,4′-CN-R-NC){Au($C_6F_4OC_nH_{2n+1}$)}$_2$]. To a solution of $HC_6F_4OC_nH_{2n+1}$ (0.09 mmol) in 25 mL of dry diethyl ether was added a solution of LiBu^n in hexane (0.56 mL, 0.09 mmol) at −78 °C under nitrogen. After stirring for 1 h at −50 °C, solid [AuCl(tht)] (0.29 g, 0.09 mmol) was added at −78 °C, and the reaction mixture was slowly brought to room temperature (3 h). Then, a few drops of water were added and the solution was filtered in air through anhydrous $MgSO_4$. CN-R-NC (0.045 mmol) was added to the solution obtained. After stirring for 15 min, the solvent was removed on a rotary evaporator, and the brown solid obtained was recrystallized from dichloromethane/hexane at −15 °C to give a microcrystalline white solid.

Yields, IR, analytical data, and representative ^1H and ^{19}F NMR follow below. When NMR data are not given, these are practically identical to those provided for similar complexes (except the ^1H NMR spectra which differ in the intensity of the multiplet comprising the undefined hydrogen atoms of the alkoxy chains, which is in each case proportional to their number).

R = 1,4-Phenylene; *n* = 8. Yield: 70%. IR $\nu(C{\equiv}N)$/cm^{-1}: (CH_2Cl_2) 2219, (Nujol) 2215. ^1H NMR ($CDCl_3$): δ 7.73 (s, 4H, aromatics), 4.13 (t, 4H, $J = 6.6$, $-O-CH_2$-), 1.77−0.85 (m, 30H, alkoxy chains). ^{19}F NMR ($CDCl_3$): δ_1 −118.19, δ_2 −157.15, AA′XX′ spin system ($^3J_{1,2} + {}^5J_{1,2'} = 18.1$ Hz, $^4J_{1,1'} + {}^4J_{2,2'} = 6.2$ Hz,). Anal. Calcd for $C_{36}H_{38}Au_2F_8N_2O_2$: C, 40.16; H, 3.56; N, 2.60. Found: C, 40.09; H, 3.60; N, 2.75.

R = 2,2′-Dichloro-4,4′-biphenylene. *n* = 4. Yield: 77%. IR $\nu(C{\equiv}N)$/cm^{-1}: (CH_2Cl_2) 2215, (Nujol) 2214. ^1H NMR ($CDCl_3$): δ_A 7.77, $\delta_M = 7.60$, $\delta_X = 7.45$, AMX spin system ($J_{AM} = 2.0$ Hz, $J_{MX} = 8.4$ Hz), 4.16 (t, 4H, $J = 6.6$, $-O-CH_2$-), 1.79−0.90 (m, 9H, alkoxy chains). ^{19}F NMR ($CDCl_3$): δ_1 −118.25, δ_2 −157.36, AA′XX′ spin system ($^3J_{A,B} + {}^5J_{A,B'} = 18.0$ Hz, $^4J_{A,A'} + {}^4J_{B,B'} =$ 6.5 Hz). Anal. Calcd for $C_{34}H_{24}Au_2Cl_2F_8N_2O_2$: C, 36.81; H, 2.18; N, 2.52. Found: C, 36.84; H, 2.15; N, 2.24.

***n* = 6.** Yield: 57%. IR $\nu(C{\equiv}N)$/cm^{-1}: (CH_2Cl_2) 2216, (Nujol) 2218. Anal. Calcd for $C_{38}H_{32}Au_2Cl_2F_8N_2O_2$: C, 39.16; H, 2.72; N, 2.52. Found: C, 36.84; H, 2.15; N, 2.24.

***n* = 8.** Yield: 65%. IR $\nu(C{\equiv}N)$/cm^{-1}: (CH_2Cl_2) 2217, (Nujol) 2215. Anal. Calcd for $C_{42}H_{40}Au_2Cl_2F_8N_2O_2$: C, 41.30; H, 3.30; N, 2.29. Found: C, 41.45; H, 3.08; N, 3.88.

***n* = 10.** Yield: 40%. IR $\nu(C{\equiv}N)$/cm^{-1}: (CH_2Cl_2) 2216, (Nujol) 2218. Anal. Calcd for $C_{46}H_{48}Au_2Cl_2F_8N_2O_2$: C, 43.24; H, 3.78; N, 2.19. Found: C, 43.21; H, 3.78; N, 2.08.

R = 2,2′-Dimethyl-4,4′-biphenylene. *n* = 4. Yield: 42%. IR $\nu(C{\equiv}N)$/cm^{-1}: (CH_2Cl_2) 2218, (Nujol) 2214. ^1H NMR ($CDCl_3$): δ_A 7.51, $\delta_M = 7.48$, $\delta_X = 7.23$, AMX spin system ($J_{AM} = 1.5$ Hz, $J_{MX} = 8.0$ Hz), 4.16 (t, 4H, $J = 6.6$, $-O-CH_2$-), 2.12 (s, 3H, CH3), 1.79−0.90 (m, 9H, alkoxy chains). ^{19}F NMR ($CDCl_3$): δ_1 −118.25, δ_2 −157.36, AA′XX′ spin system ($^3J_{A,B} + {}^5J_{A,B'} = 17.9$ Hz, $^4J_{A,A'}$ + $^4J_{B,B'} = 5.9$ Hz). Anal. Calcd for $C_{36}H_{30}Au_2F_8N_2O_2$: C, 40.46; H, 2.83; N, 2.62. Found: C, 40.80; H, 2.87; N, 2.80.

***n* = 6.** Yield: 46%. IR $\nu(C{\equiv}N)$/cm^{-1}: (CH_2Cl_2) 2217, (Nujol) 2208. Anal. Calcd for $C_{40}H_{38}Au_2F_8N_2O_2$: C, 42.72; H, 3.40; N, 2.49. Found: C, 42.60; H, 3.39; N, 2.56.

***n* = 8.** Yield: 55%. IR $\nu(C{\equiv}N)$/cm^{-1}: (CH_2Cl_2) 2217, (Nujol) 2211. Anal. Calcd for $C_{44}H_{46}Au_2F_8N_2O_2$: C, 44.76; H, 3.93; N, 2.37. Found: C, 44.63; H, 3.95; N, 2.32.

***n* = 10.** Yield: 55%. IR $\nu(C{\equiv}N)$/cm^{-1}: (CH_2Cl_2) 2218, (Nujol) 2214. Anal. Calcd for $C_{48}H_{54}Au_2F_8N_2O_2$: C, 46.61; H, 4.41; N, 2.26. Found: C, 46.30; H, 4.21; N, 2.33.

R = 4,4′-Biphenylene. *n* = 4. Yield: 45%. IR $\nu(C{\equiv}N)$/cm^{-1}: (CH_2Cl_2) 2214, (Nujol) 2212. ^1H NMR ($CDCl_3$): δ 7.73 (m, 8H, aromatics), AA′BB′ spin system ($\delta_A \approx \delta_B$), 4.17 (t, 4H, $J = 6.4$, $-O-CH_2$-), 1.77−0.90 (m, 9H, alkoxy chains). ^{19}F NMR ($CDCl_3$): δ_A −118.29, δ_B −157.34, AA′XX′ spin system ($^3J_{A,B}$ + $^5J_{A,B'} = 17.9$ Hz, $^4J_{A,A'} + {}^4J_{B,B'} = 6.3$ Hz). Anal. Calcd for $C_{34}H_{26}Au_2F_8N_2O_2$: C, 39.25; H2.52; N, 2.69. Found: C, 39.14; H, 2.56; N, 2.55.

***n* = 6**: Yield: 50%. IR $\nu(C{\equiv}N)$/ cm^{-1}: (CH_2Cl_2) 2214, (Nujol) 2209. Anal. Calcd for $C_{38}H_{34}Au_2F_8N_2O_2$: C, 41.62; H, 3.13; N, 2.55. Found: C, 42.10; H, 3.22; N2.53.

***n* = 8**: Yield: 85%. IR $\nu(C{\equiv}N)$/ cm^{-1}: (CH_2Cl_2) 2214, (Nujol) 2211. Anal. Calcd for $C_{42}H_{42}Au_2F_8N_2O_2$: C, 43.76; H, 3.67; N, 2.43. Found: C, 43.69; H, 3.65; N, 2.01.

***n* = 10**: Yield: 45%. IR $\nu(C{\equiv}N)$/cm^{-1}: (CH_2Cl_2) 2214, (Nujol) 2216. Anal. Calcd for $C_{46}H_{50}Au_2F_8N_2O_2$: C, 45.71; H, 4.17; N, 2.32. Found: C, 45.60; H, 4.13; N, 2.07.

Experimental Procedure for X-ray Crystallography. Crystals of [μ-(4,4′-CN-R-NC){Au($C_6F_4OC_4H_9$)}$_2$] (R = 4,4′-biphenylene and 2,2′dichloro-4-4′-biphenylene) were obtained by direct diffusion of hexane into a solution of the complex in dichloromethane. Suitable single crystals were mounted in glass fibers, and diffraction measurements were made using a Bruker SMART CCD area-detector diffractometer with Mo Kα radiation ($\lambda = 0.71073$ Å).[31] Intensities were integrated from several series of exposures, each exposure covering 0.3° in ω, the total data set being a hemisphere.[32] Absorption corrections were applied based on multiple and symmetry-equivalent measurements.[33] The structure was solved by Patterson synthesis or direct methods and refined by least squares on weighted F^2 values for all reflections (see Table 1).[34] All non-hydrogen atoms were assigned anisotropic displacement parameters and refined without positional constraints. Hydrogen atoms were taken into account at calculated positions, and their positional parameters were refined. Complex neutral-atom scattering factors were used.[35] Crystallographic data (excluding structure factors) for the structures reported in this paper have been

---

(30) Ugi, I.; Fetzer, U.; Knupfer, H.; Offermann, K. *Angew. Chem., Int. Ed. Engl.* **1965**, *4*, 472.

(31) *SMART V5.051 Diffractometer Control Software*; Bruker Analytical X-ray Instruments Inc.: Madison, WI, 1998.

(32) *SAINT V6.02 Integration Software*; Bruker Analytical X-ray Instruments Inc.: Madison, WI, 1999.

(33) Sheldrick, G. M. *SADABS: A program for absorption correction with the Siemens SMART system*; University of Göttingen: Göttingen, Germany, 1996.

(34) *SHELXTL program system version 5.1*; Bruker Analytical X-ray Instruments Inc.: Madison, WI, 1998.

(35) *International Tables for Crystallography*; Kluwer: Dordrecht, 1992; Vol. C.

Table 1. X-ray Data and Data Collection and Refinement Parameters for [μ-(4,4′-CN-R-NC){Au($C_6F_4OC_4H_9$)}$_2$] (R = 4,4′-Biphenylene and 2,2′-Dichloro-4,4′-biphenylene)

empirical formula	$C_{34}H_{26}Au_2F_8N_2O_2$	$C_{34}H_{24}Au_2Cl_2F_8N_2O_2$
fw	1040.50	1109.39
cryst syst	monoclinic	monoclinic
space group	$P2_1/c$	$P2_1/n$
a (Å)	12.052(3)	14.007(5)
b (Å)	16.387(4)	10.607(4)
c (Å)	16.981(4)	24.343(9)
β (deg)	91.881(5)	103.275(8)
V (Å^3)	3351(13)	3520(2)
Z	4	4
D_{calcd} (g/cm^{-3})	2.062	2.093
abs coeff (mm^{-1})	8.822	8.555
F(000)	1960	2088
cryst size (mm^3)	0.23 × 0.08 × 0.03	0.12 × 0.07 × 0.02
temp (K)	297(2)	298(2)
θ range for data collcn (deg)	1.69-23.28	1.54-23.26
wavelength (Å)	0.71073	0.71073
index ranges	$-13 \leq h \leq 13, 0 \leq k \leq 18, 0 \leq l \leq 18$	$-15 \leq h \leq 15, 0 \leq k \leq 11, 0 \leq l \leq 26$
reflns collected	15627	16411
indep reflns	4812 [$R_{int} = 0.0403$]	5037 [$R_{int} = 0.0460$]
completeness to θ	23.28 (99.6%)	23.26 (99.5%)
abs corr	SADABS	SADABS
max and min transm	1.000000 and 0.506552	1.000000 and 0.544350
data/restraints/params	4812/0/435	5037/0/453
goodness-of-fit on F^2	0.936	1.000
final R indices [$I > 2\sigma(I)$]	R1 = 0.0292, wR2 = 0.0597	R1 = 0.0346, wR2 = 0.0800
R indices (all data)	R1 = 0.0504, wR2 = 0.0645	R1 = 0.0688, wR2 = 0.0963
largest diff. peak and hole (e Å^{-3})	0.963 and −0.484	1.331 and −0.623

deposited as Supporting Information, and with the Cambridge Crystallographic Data Centre as supplementary publication with the following deposition numbers: CCDC-605387 for [μ-(4,4′-CN-C_6H_4-C_6H_4-NC){Au($C_6F_4OC_4H_9$)}$_2$] and CCDC-605388 for [μ-(4,4′-CN-C_6H_3Cl-C_6H_3Cl-NC){Au($C_6F_4OC_4H_9$)}$_2$]. Copies of the data can be obtained free of charge on application to the CCDC, 12 Union Road, Cambridge CB2 1EZ, U.K. [fax (international) +44-1223/336-033; e-mail deposit@ccdc.cam.ac.uk].

Results and Discussion

Synthesis and Characterization. The isocyanides, 4,4′-diisocyano-2,2′-dichlorobiphenyl and 4,4′-diisocyano-2,2′-dimethylbiphenyl, have not been reported before and were prepared starting from the corresponding dinitrobiphenyl compounds in three steps, involving reduction to the diamines H_2NRNH_2 by hydrazine/graphite, formylation to their *N*-diformamides, and finally dehydration with bis(trichloromethyl)carbonate ("triphosgene") and triethylamine to the diisocyanides CN-R-NC, as summarized in Scheme 1. None of the free isocyanide ligands prepared and used in this work show liquid crystal behavior. At room temperature they are white solids, not particularly smelling, that can be stored for long periods in the freezer.

The gold(I) isocyanide complexes were prepared as described in the literature for mononuclear fluorophenyl−gold(I) isocyanide derivatives,[23,25] as depicted in Scheme 1 (tht = tetrahydrothiophene). The compounds [(μ-4,4′-CN-R-NC){Au($C_6F_4OC_nH_{2n+1}$)}$_2$] [R = 2,2′-dichloro-4,4′-biphenylene, 2,2′-dimethyl-4,4′-biphenylene, 4,4′-biphenylene; n = 4,6,8,10; R = 1,4-phenylene, n = 8] were obtained by arylation of [AuCl(tht)] followed by ligand exchange of tht with the appropriate isocyanide ligand. They were isolated as white solids. The biphenyl moiety is not planar, and the complexes with 2,2′-dichlorobiphenylene and 2,2′-dimethylbiphenylene contain an asymmetric biphenyl core. The rotational barriers for these biphenyl moieties are reasonably high.[36] This means that the compounds should be racemic mixtures, at least in the solid state.

Scheme 1[a]

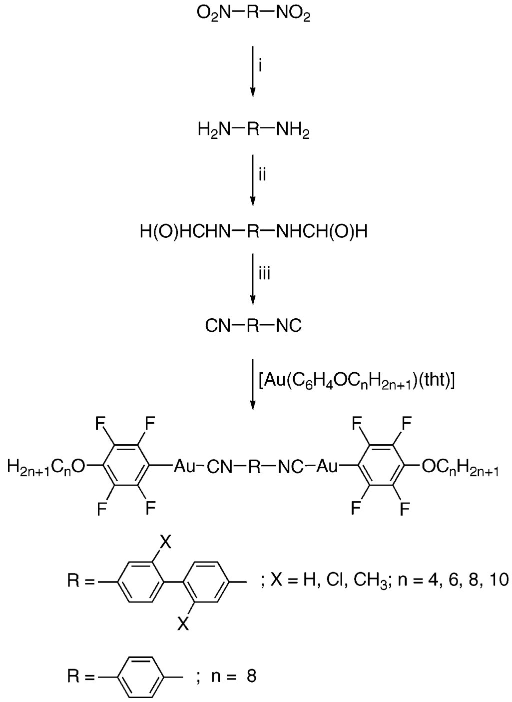

[a] Reagents: i, N_2H_4−graphite; ii, HCO_2H; iii, $(Cl_3CO)_2CO$, Et_3N.

The C, H, N analyses for the complexes, yields, and relevant IR data are given in the Experimental Section. The IR spectra are all similar and show one ν(C≡N) absorption for the isocyanide group at higher wavenumbers (ca. 90 cm^{-1}) than for the free ligands, as reported for other gold(I)

---

(36) Leroux, F. *ChemBioChem* **2004**, *5*, 644.

Table 2. Selected Bond Distances (Å) and Angles (deg) within Molecules [μ-(4,4′-CN-R-NC){Au($C_6F_4OC_4H_9$)}$_2$]

	R = C_6H_4-C_6H_4	R = C_6H_3Cl-C_6H_3Cl
Au(1)−C(1)	1.958(8)	1.984(11)
Au(1)−C(21)	2.031(6)	2.046(9)
C(1)−(N(1)	1.131(8)	1.137(11)
Au(2)−C(2)	1.987(9)	1.969(10)
Au(2)−C(31)	2.026(7)	2.023(9)
N(2)−C(2)	1.137(8)	1.155(11)
C(1)−Au(1)−C(21)	177.5(3)	175.7(4)
N(1)−C(1)−Au(1)	177.6(7)	176.6(9)
N(2)−C(2)−Au(2)	178.1(8)	177.5(9)
C(2)−Au(2)−C(31)	179.3(3)	175.7(4)

isocyanide compounds.[23,25] The ^{1}H NMR spectra of the metal complexes are all very similar for each family. Thus, at 300 MHz the 4,4′-diisocyano-2,2′-dichlorobiphenyl and 4,4′-diisocyano-2,2′-dimethylbiphenyl complexes show similar spectra, displaying three resonances from aromatic protons (AMX spin systems), as expected. The 4,4′-diisocyano-2,2′-dimethylbyphenyl complexes display also a singlet from the 2- and 2′-methyl groups, at 2.03 ppm. In addition, one triplet is observed at ca. 4.1 ppm corresponding to the first methylene group of the $C_6F_4OC_nH_{2n+1}$ moiety. The remaining chain hydrogen atoms appear overlapped in the range 0.8−1.8 ppm. The ^{1}H NMR spectrum of 4,4′-diisocyanobiphenyl shows two somewhat distorted “pseudodoublets” (a deceptively simple pattern for the AA′XX′ spin system with $\delta_A \approx \delta_B$) for the biphenyl group present in the molecule. The ^{1}H NMR spectra of 1,4-isocyanobenzene complexes show one signal for aromatic protons, as expected.

The ^{19}F NMR spectra of these complexes show two somewhat distorted “doublets” flanked by two pseudotriplets corresponding to an AA′XX′ spin system with $J_{AA'} \approx J_{XX'}$. The signals appear at ca. −118 ppm and ca. −157 ppm (ref $CFCl_3$), assigned to F(*ortho*) and F(*meta*), respectively, with apparent coupling constants ($N = J_{AX} + J_{AX'}$) of 18.0 Hz, as reported for mononuclear tetrafluorophenylgold(I) isocyanide complexes.

X-ray Crystallography. Compounds [μ-(4,4′-CN-R-NC)-{Au($C_6F_4OC_4H_9$)}$_2$] (R = 4,4′-biphenylene and 2,2′-dichloro-4,4′-biphenylene) have been characterized by X-ray diffraction. The crystal data and experimental details are given in the Experimental Section and in Table 1.

[μ-(4,4′-CN-C_6H_4-C_6H_4-NC){Au($C_6F_4OC_4H_9$)}$_2$]. The compound crystallizes in the monoclinic space group $P2_1/c$, with 4 formula units per unit cell. The gold atoms are linearly coordinated by the diisocyanide ligand and tetrafluorophenyl groups. Bond angles and bond lengths fall within normal ranges (Table 2). The two rings of the biphenylisocyanide system make a dihedral angle of 28.3°. The butoxy chains are extended, and the molecule takes a rodlike shape. The crystal packing of the complex shows stacking of molecules in a parallel disposition, but each molecule is slightly shifted from the previous, so that the shortest intermolecular distance observed is 3.56 Å, between one F_{meta} and a gold atom of neighboring molecules (Figure 1). Considering that the sum of the van der Waals radius of gold and fluorine is 3.05 Å,[37] the intermolecular Au$\cdots$$F_{meta}$ distance observed would exclude the existence of any covalent Au$\cdots$F interaction, but not the contribution of an electrostatic interaction at the exclusion distance of the aryl rings. This might be the reason for the zigzag arrangement of the stacking (Figure 2).

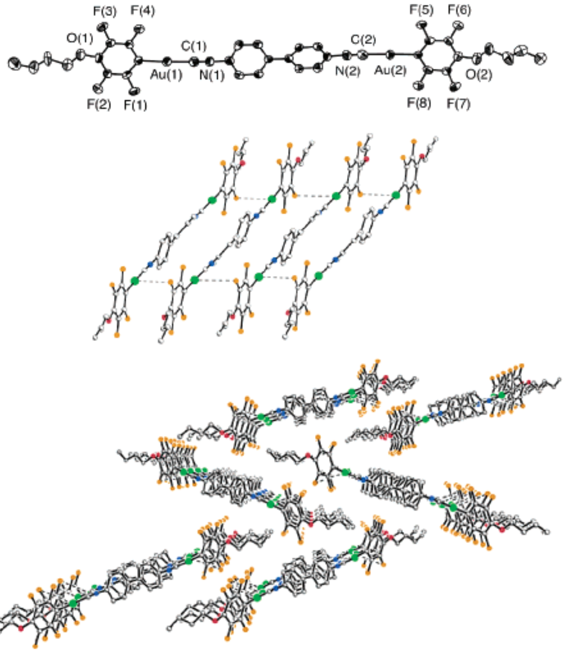

Figure 2. (Top) Molecular ORTEP for [μ-(4,4′-CN-C_6H_4-C_6H_4-−NC)-{Au($C_6F_4OC_4H_9$)}$_2$] and zigzag molecular arrangement. (Middle) View of one sequence of molecules showing the $F_{meta}$$\cdots$Au short distances. (Bottom) View of the arrangement of these zigzag sequences.

[μ-(4,4′-CN-C_6H_3Cl-C_6H_3Cl-NC){Au($C_6F_4OC_4H_9$)}$_2$]. The compound crystallizes in the monoclinic space group $P2_1/n$, with 4 formula units per unit cell. The molecule takes a rodlike shape, as in the biphenylisocyanide derivative discussed above, but the dihedral angle between the two rings of the 2,2′-dichlorobiphenylisocyanide group is greater (104.9° considering the position of the substituents; effective angle between ring planes 75.1°), revealing in this complex a lower electronic conjugation between the phenyl rings. The crystal packing of the complex shows a molecular arrangement in planes (Figure 3, middle). Within the plane the intermolecular distances Au$\cdots$$F_{meta}$ (3.60 Å) and Au$\cdots$Cl (3.67 Å) are higher than the sum of the van der Waals radii of gold and the corresponding halogen. As discussed above, this would exclude the existence of intraplanar Au$\cdots$halogen covalent interactions, but not of electrostatic interactions. These layers produce a stacking with each plane shifted with respect to the previous (Figure 3, down). The Au$\cdots$Au distances between molecules contained in consecutive planes (3.61 Å) are suggestive of some aurophilic interactions.

It is important to note that neither [μ-(4,4′-CN-C_6H_4-C_6H_4-NC){Au($C_6F_4OC_4H_9$)}$_2$] nor [μ-(4,4′-CN-C_6H_3Cl-C_6H_3Cl-NC){Au($C_6F_4OC_4H_9$)}$_2$] adopt a layered packing of molecules in the solid state. This reluctance to adopt layered packing is in coincidence with the absence of smectic phases in their mesophases.

Mesogenic Behavior. Although none of the free ligands used in this work behave as a liquid crystal, all the

---

(37) Emsley, J. *The Elements*, 3rd ed.; Oxford University Press: New York, 2000.

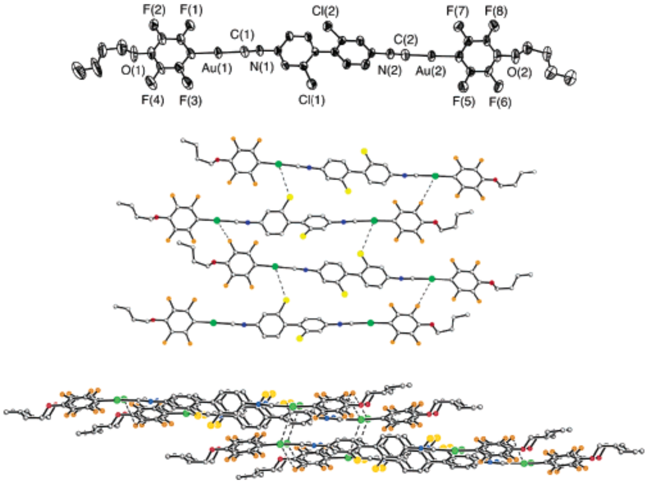

Figure 3. (Top) Molecular ORTEP for $[\mu\text{-}(4,4'\text{-CN-C}_6\text{H}_3\text{Cl-C}_6\text{H}_3\text{Cl-NC})\text{-}\{\text{Au}(\text{C}_6\text{F}_4\text{OC}_4\text{H}_9)\}_2]$ and molecular arrangement. (Middle) View of one sequence of molecules showing the halide···Au short distances. (Bottom) View of the arrangement of these molecular sequences.

Table 3. Optical, Thermal, and Thermodynamic Data for $[\mu\text{-}(4,4'\text{-CN-R-NC})\{\text{Au}(\text{C}_6\text{F}_4\text{OC}_n\text{H}_{2n+1})\}_2]$ with R = 4,4′-Biphenylene (R^1), 2,2′-Dichloro-4,4′-biphenylene (R^2), 2,2′-Dimethyl-4,4′-biphenylene (R^3), and 1,4-Phenylene (R^4)

R	n	transition[a]	temp[b] (°C)	ΔH[b] (kJ/mol)
R^1	4	Cr → N	256.0	19.4
		N → I	290[c] (dec)	
R^1	6	Cr →Cr	112.7	3.4
		Cr → N	194.5	24.8
		N → I	275[c] (dec)	
R^1	8	Cr → Cr’	114.1	5.8
		Cr’ → N	135.2	27.5
		N → I	257[c] (dec)	
R^1	10	Cr → Cr	98.1	2.1
		Cr → N	139.4	29.6
		N → I	222[c] (dec)	
R^2	4	Cr → Cr’	110.5	5.03
		C’ → N → I[d]	194.6	36.0[e]
R^2	6	N → Cr	72.2	−18.6
		Cr → Cr’	99.7	−4.3
		Cr’ → N	142.3	41.1
		N → I	170.3	0.8
R^2	8	N → Cr	65.8	−31.8
		Cr → N	150.8	38.0
		N → I	162.9	0.3
R^2	10	Cr → N	127.8	36.7
		N → I	159.2	1.3
R^3	4	Cr → N → I[d]	202.2	36.9[e]
R^3	6	I → Cr	79.0	−20.6
		Cr → N	118.4	21.9
		N → I	143.9	0.9
R^3	8	Cr → N	105.0	22.2[e]
		N → I	145.2	1.2
R^3	10	Cr → N	101.4	24.6
		N → I	130.1	0.6
R^4	8	Cr → Cr	212.0	0.5
		Cr → I	232.6	44.8

[a] Cr, crystal; N, nematic; I, isotropic liquid. [b] Data referred to the second DSC. Temperatures referred to the onset temperatures. [c] Microscopy data. [d] Data referred to the first DSC cycle starting from the crystal. [e] Combined enthalpies.

tetrafluorophenylgold compounds prepared are mesomorphic, except the derivative of 1,4-diisocyanobenzene. Their optical, thermal, and thermodynamic data are collected in Table 3. All the mesogenic gold complexes display only an N mesophase, identified in optical microscopy by the typical marbled and schlieren textures (Figure 4).[38−40] Several compounds show crystal-to-crystal transitions before melting.

Figure 4. Polarized optical microscopic texture (×100) observed for $[\mu\text{-}(4,4'\text{-CN-C}_6\text{H}_3\text{Cl-C}_6\text{H}_3\text{Cl-NC})\{\text{Au}(\text{C}_6\text{F}_4\text{OC}_6\text{H}_{13})\}_2]$. The picture shows the marbled texture of the N phase, at 152 °C on heating from the crystal.

The variation in thermal properties can be summarized as follows: The clearing temperatures decrease with increasing length of the alkoxy chain, and in the order phenyl > biphenyl > 2,2′-dichlorobiphenyl > 2,2′-dimethylbiphenyl. The same trend is observed for the melting temperatures with one exception, the octyloxy-2,2′-dichlorobiphenylene compound, which shows the highest melting point of the octiloxybiphenyl derivatives.

The simplest way to look at the rodlike molecules containing a biphenyl moiety, $[\mu\text{-}(4,4'\text{-CN-R-NC})\{\text{Au}(\text{C}_6\text{F}_4\text{OC}_n\text{H}_{2n+1})\}_2]$ [R = 2,2′-dichloro-4,4′-biphenylene, 2,2′-dimethyl-4,4′-biphenylene, 4,4′-biphenylene; n = 4,6,8,10; R = 1,4-phenylene, n = 8], is to consider them as formal derivatives of $[\mu\text{-}(4,4'\text{-CN-C}_6\text{H}_4\text{C}_6\text{H}_4\text{-NC})\{\text{Au}(\text{C}_6\text{F}_4\text{OC}_n\text{H}_{2n+1})\}_2]$ by substitution of a H atom by a Cl or a CH_3 group in the 2 and 2′ positions of the biphenyl system, which will determine the magnitude of intermolecular electrostatic interactions. In general, more planar molecules should lead to more compact packing and stronger interactions than nonplanar molecules. Theoretical studies have shown that, for biphenyl systems, the substituents in 2 and 2′ positions determine the twist angle of the biphenyl in the gas phase, as well as its rotational barrier. Both increase in the order H ≪ Cl < Me.[36] This trend is supported by the two X-ray structures determined here (H/H twist angle = 28.3°; Cl/Cl twist angle = 104.9°, equivalent to 75.1° between planes). Surprisingly this trend is the same as that observed for the variation in melting and clearing temperatures experimentally observed for the biphenyl compounds (H/ H-biphenyl > Cl/Cl-biphenyl > Me/Me-biphenyl), despite their different solid-state structures and bond dipoles (C−H, C−Me, C−Cl) in the biphenyls, suggesting that the molecular packing in the melt (and hence the properties of the bulk material) is still strongly influenced by the higher

---

(38) Demus, D.; Richter, L. *Textures of liquid crystals*, 2nd ed.; VEB: Leipzig, 1980; p 790.

(39) Gray, G. W.; Goodby, J. W. *Smectic liquid crystals. Textures and Structures*; Hill: London, 1984.

(40) Dierking, I. *Textures of liquid Crystals*; Wiley-VCH: Weinheim, 2003.

Table 4. UV−Vis Data in Dichloromethane Solution of the Free Isocyanides and the Complexes $[\mu\text{-}(4,4'\text{-CN-R-NC})\{Au(C_6F_4OC_4H_9)\}_2]$ with R = 4,4′-Biphenylene (**R**^{1}), 2,2′-Dichloro-4,4′-biphenylene (**R**^{2}), and 2,2′-Dimethyl-4,4′-biphenylene (**R**^{3})

R or compd	λ/nm (ϵ)/dm^3 mol^{-1} cm^{-1}
R^{1a}	228 (6000), 272 (24000)
R^{2a}	241 (47000)
R^{3a}	243 (27500)
$H_9C_4OC_6H_4H$	230 (1000), 262 (500)
R^1	228 (29000), 297 (70500)
R^2	229 sh (46000),^{b} 260 (49000), 283 sh (44500)^b
R^3	259 (50000), 280 (52500)

^{a} Free isocyanide ligands. ^{b} Apparent molar absorptivity.

or lower nonplanarity of the individual molecules. Yet, the rather high transition temperatures found suggest the existence of fairly good intermolecular interactions, as expected from large multipolar molecules even if the efficiency of packing has been relaxed. However, only the phase of lower disordered, N, is observed. The crystal packing of the 4,4′-biphenylene and the 2,2′-dichloro-4,4′-biphenylene derivatives shows, in both cases, a nonlayered structure confirming that, in this type of symmetric dimers, the best multipole−multipole interactions is achieved in packings with some mixing of aromatic and aliphatic regions, hence giving a nonlayered structure. For this reason, only the nematic mesophase is obtained.

It is worth mentioning that only $[\mu\text{-}(4,4'\text{-CN-}C_6H_4\text{-NC})\{Au(C_6F_4OC_nH_{2n+1})\}_2]$, with a flat rigid core and showing the highest melting point, is not mesogenic. This supports the idea that, in the case of strong intermolecular multipolar interactions, the molecules have to be designed so as to preclude much too efficient molecular packing in order to obtain mesogenic behavior. While this conclusion seems clear, the good coincidence of variation of transition temperatures with the expected rotational angles is somewhat surprising, considering that the molecules involve substituents as different as Cl and H or Me.

Photophysical Studies. The electronic spectra of free isocyanides and some representative gold(I) complexes are summarized in Table 4. The free isocyanides show a strong UV absorption in the range 241−272 nm which is assigned to a $\pi-\pi^*$ transition in the biphenyl system (K-band).[41] This absorption in the biphenyl system undergoes a noticeable bathochromic shift upon complexation of the isocyanide ligand to give the gold complexes, as reported for analogous complexes $[AuX(CNC_6H_4C_6H_4OC_{10}H_{21})]$ (X = Cl, Br, I),[41] [AuX(CN(*o*-xylyl)],[42] and $[Au(C_6F_4OC_nH_{2n+1})(CNC_6H_4C_6H_4\text{-}OC_{10}H_{21})]$.[20] Moreover, it is interesting to note that the largest molar absorptivity for free isocyanide ligands is that of the 2,2-dichloro derivative in accordance with the presence of a strong auxochromic group (Cl) in the aromatic rings.[43] In contrast, in the gold complexes, which have a higher electronic density available for interaction with the π-electron system of the aromatic ring than the free isocyanide ligands, the effect of the auxochromic group would be lower, and the largest molar absorptivity is that of biphenyl derivative according to the smaller twist angle between the two aromatic rings (28.3°) and consequently greater delocalization of electrons over the biphenyl systems in this complex.

Table 5. Emission and Excitation Maxima (in nm) for Free Isocyanide Ligands and Complexes $[\mu\text{-}(4,4'\text{-CN-R-NC})\{Au(C_6F_4OC_4H_9)\}_2]$ with R = 4,4′-Biphenylene (**R**^{1}), 2,2′-Dichloro-4,4′-biphenylene (**R**^{2}), and 2,2′-Dimethyl-4,4′-biphenylene (**R**^{3}) at 298 K

	KBr		CH_2Cl_2	
R	λ_{ex}	λ_{em}	λ_{ex}	λ_{em}
R^{1a}			247	314, 325
R^{2a}			340	448
R^{3a}			259	323
R^1	340	496, 532	328	491,^{b} 524
R^2	348	519	312	454
R^3	334	480, 510	301	452,^{b} 480

^{a} Free isocyanide ligands. ^{b} Emission band exhibiting vibronic progression. For the compound with R^1, a third peak seems to merge as a shoulder at about 560 nm.

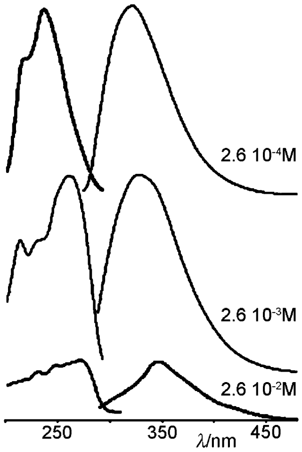

Figure 5. Luminescence excitation and emission spectra of 2,2′-dimethyl-4,4′-biphenyldiisocyanide in dichloromethane solution at different concentrations.

The luminescence spectroscopic data of three representative gold complexes and the free isocyanide ligands are listed in Table 5. The free isocyanides are luminescent at room temperature in dichloromethane solution and show similar emission spectra consisting of a broad emission band in the region 314−448 nm. In the solid state (KBr pellets), the emission is lost. The luminescent behavior of 4,4′-diisocyano-2,2′-dimethylbiphenyl in dichloromethane solution as a function of concentration is shown in Figure 5. As the concentration is gradually increased from 10^{-4} to 10^{-2} M, the intensity of the emission band at 323 nm decreases and shifts to lower energy. The emission is lost at higher concentration. This behavior suggests the formation of an excimer or excimerlike adduct, as observed frequently in aromatic compounds.[44]

It is important to note that with time and manipulation at room temperature these isocyanides develop a cream color, probably due to partial polymerization. Despite still showing

---

(41) Benouazzane, M.; Coco, S.; Espinet, P.; Martín-Álvarez, J. M. *J. Mater. Chem.* **1995**, *5*, 441.

(42) Ecken, H.; Olmstead, M. M.; Noll, B. C.; Attar, S.; Schlyer, B.; Balch, A. L. *Dalton Trans*. **1998**, 3715.

(43) Silverstein, R. M.; Bassler, G. C.; Morrill, T. C. *Spectrometric Identification of Organic Compounds*, 5th ed.; John Wiley & Sons: Singapore,1991; Chapter 7.

(44) Birks, J. B. *Photophysics of Aromatic Molecules*, John-Wiley: London, 1970.

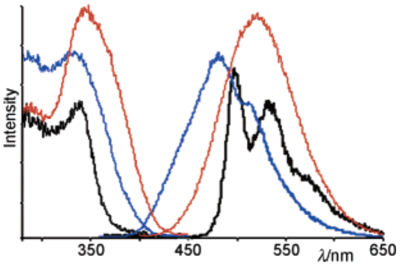

Figure 6. Luminescence excitation and emission spectra in the solid state (KBr pellets) of [μ-(4,4′-CN-R-NC){Au($C_6F_4OC_4H_9$)}$_2$] with R = 4,4′-biphenylene (**R**^{1}) (black), 2,2′-dichloro-4,4′-biphenylene (**R**^{2}) (red), and 2,2′-dimethyl-4,4′-biphenylene (**R**^{3}) (blue) at 298 K.

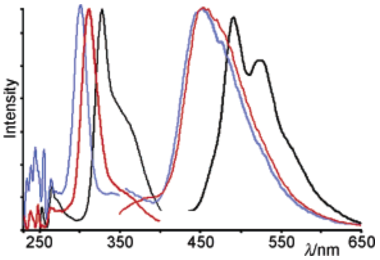

Figure 7. Luminescence excitation and emission spectra in dichloromethane solution of [μ-(4,4′-CN-R-NC){Au($C_6F_4OC_4H_9$)}$_2$] with R = 4,4′biphenylene (**R**^{1}) (black), 2,2′-dichloro-4,4′biphenylene (**R**^{2}) (red), and 2,2′-dimethyl-4,4′-biphenylene (**R**^{3}) (blue) at 298 K.

no extra signals in the ^{1}H NMR spectrum, these cream samples display in the emission spectra an additional weak luminescence at 383 nm (λ_{exc} = 324 nm), for which the intensity does not change significantly with concentration.

The dinuclear gold compounds are luminescent at room temperature, both in solution and in the solid state (Table 5 and Figures 6 and 7). In the solid state they exhibit a yellow-green luminescence visually observed under UV irradiation at 365 nm. The emission spectra of the 4,4′-diisocyano-2,2′-biphenyl and 4,4′-diisocyano-2,2′-dimethylbiphenyl gold complexes show a structured emission band in the region 452−532 nm. The energy difference between neighboring vibronic peaks is close to 1300 cm^{-1} suggesting a vibronic progression typical of C−C aromatic stretchings, which is consistent with $\pi-\pi^*$ ligand-centered transitions. In contrast, the 2-2′-dichlorobiphenyl gold complex displays a broad structureless emission, even at 77 K.

In general, biphenyl systems with low twist angles between the two aromatic rings, and consequently high conjugation in the aromatic biphenyl core, show stabilization of π^* states.[45] Thus, it is not unexpected that the 4,4′-diisocyano-biphenyl gold complex, that shows the lower twist angle between the two aromatic ring (28.3°) in the series of gold complexes studied, displays lower energy emission bands, in accordance to the absorption UV spectrum discussed above. The lifetimes in the solid state have been measured for the 4,4′-diisocyano-2,2′-biphenyl gold complex.[46] Both vibronic peaks at 496 and 532 nm show, as expected, the same (within experimental error) lifetimes (187 and 175 μs, respectively). The rather long value supports a phosphorescent nature for the emission. A similar behavior is obtained for the peaks at 480 nm (120 μs) and 510 nm (128 μs) for the 4,4′-diisocyano-2,2′-dimethylbiphenyl gold derivative and for the 2,2′-dichlorobiphenylene gold derivative (20 μs). In degassed dichloromethane solution at room temperature, the gold complexes show similar luminescence spectra with quantum yields of 0.001 for both 2,2′-dimethylbiphenyl and biphenyl gold complexes, and 0.002 for the 2,2′-dichlorobiphenyl gold derivative. These low quantum yields can be explained considering that, due to the long radiative lifetimes of phosphorescent emissions, their quenching is especially important in fluid media (solution), where collisions are frequent. For [μ-(4,4′-CN-C_6H_3Cl-C_6H_3Cl-NC){Au(C_6F_4-OC_4H_9)}$_2$], there is a clear red shift on going from solution to the solid state. This effect is usually observed in the emission spectra of gold(I) complexes and is attributed to the presence of intermolecular Au···Au or π-stacking interactions.[47] Considering that our chloro complex [μ-(4,4′-CN-C_6H_3Cl-C_6H_3Cl-NC){Au($C_6F_4OC_4H_9$)}$_2$] shows Au···Au intermolecular interactions in the solid state, and its emission band is structureless, we conclude that its luminescence corresponds to excimerlike phosphorescence in the solid state, and to ligand-localized monomer phosphorescence in solution. In contrast, in [μ-(4,4′-CN-C_6H_4-C_6H_4-NC){Au(C_6F_4-OC_4H_9)}$_2$], the emission band is structured, the red shift on going from solution to the solid state is insignificant, and there are no Au···Au or π-stacking interactions. Thus, the emission band is assigned as ligand-localized monomer phosphorescence both in the solid state and in solution. For [μ-(4,4′-CN-$C_6H_3CH_3$-$C_6H_4CH_3$-NC){Au($C_6F_4OC_4H_9$)}$_2$], we do not have an X-ray structure, and consequently, we cannot structurally ascertain that Au···Au or π-stacking interactions exist. However, considering that its structured luminescence profile is similar to that of [μ-(4,4′-CN-C_6H_4-C_6H_4-NC)-{Au($C_6F_4OC_4H_9$)}$_2$], it is reasonable to assign its emission behavior as ligand-localized monomer phosphorescence both in the solid state and solution.

In summary, we have found a new system, based on dinuclear gold complexes with biphenyl isocyanides, which shows luminescence properties and also liquid crystal behavior. This kind of system is promising to obtain a delicate tuning of properties by changing the dihedral angle between the two aromatic rings of the biphenyl group.

Acknowledgment. This work was sponsored by the Dirección General de Investigación (Project CTQ2005-08729/BQU) and the Junta de Castilla y León (Project VA099A05).

Supporting Information Available: Crystallographic data in CIF format for [μ-(4,4′-CN-C_6H_3Cl-C_6H_3Cl-NC){Au($C_6F_4OC_4H_9$)}$_2$] and [μ-(4,4′-CN-C_6H_4-C_6H_4-NC){Au($C_6F_4OC_4H_9$)}$_2$]. This material is available free of charge via the Internet at http://pubs.acs.org.

IC060702A

---

(45) Leslie, W.; Batsanov, A. S.; Howard, J. A. K.; Williams, J. A. G. *Dalton Trans.* **2004**, 623.

(46) Wayne, C. E.; Wayne, R. P. *Photochemistry*, Oxford University Press: New York, 1996.

(47) Brandys M.-C.; Jenning, M. C.; Puddephatt, R. J. *Dalton Trans.* **2000**, 4601.